

Frequency- and electric-field-dependent conductivity of single-walled carbon nanotube networks of varying density

Hua Xu,* Shixiong Zhang, and Steven M. Anlage

Center for Nanophysics and Advanced Materials, Department of Physics, University of Maryland, College Park, Maryland 20742-4111, USA

Liangbing Hu and George Grüner

Department of Physics, University of California, Los Angeles, California 90095, USA

(Received 8 October 2007; published 20 February 2008)

We present measurements of the frequency- and electric-field-dependent conductivity of single-walled carbon nanotube (SWCNT) networks of various densities. The ac conductivity as a function of frequency is consistent with the extended pair approximation model and increases with frequency above an onset frequency ω_0 which varies over seven decades with a range of film thickness from submonolayer to 200 nm. The nonlinear electric-field-dependent dc conductivity shows strong dependence on film thickness as well. Measurement of the electric field dependence of the resistance $R(E)$ allows for the determination of a length scale L_E possibly characterizing the distance between tube contacts, which is found to systematically decrease with increasing film thickness. The onset frequency ω_0 of ac conductivity and the length scale L_E of SWCNT networks are found to be correlated, and a physically reasonable empirical formula relating them has been proposed. Such studies will help the understanding of transport properties and benefit the applications of this material system.

DOI: [10.1103/PhysRevB.77.075418](https://doi.org/10.1103/PhysRevB.77.075418)

PACS number(s): 73.63.Fg, 72.80.Ng

I. INTRODUCTION

Networks with randomly distributed single-walled carbon nanotubes (SWCNTs) are emerging as novel materials for various applications, particularly as electronic materials.¹⁻⁴ This creates a need for the accurate determination of their fundamental electrical properties.

SWCNT networks can be viewed as a two-dimensional network of conducting one-dimensional rods.⁵ These rods are either metallic or semiconducting with large dimension ratio (length/diameter ~ 1000), which leads to the following interesting behavior.^{6,7} Since the nanotube-nanotube junction resistance is much larger than the nanotube resistance itself,⁷⁻⁹ such a network can be seen as a system with randomly distributed barriers for electrical transport. For a submonolayer network, the junction resistance will dominate the overall resistance and the network resistance shows percolation behavior with nonlinear thickness dependence.^{5,9} For SWCNT networks with thickness in tens of nanometers, e.g., with tens of layers of SWCNTs, the conductance through the metallic tubes will dominate the conduction and lead to metallic behavior of the overall resistance.¹⁰⁻¹²

The frequency-dependent and electric-field-dependent conductivity has been investigated for individual SWCNTs¹³⁻¹⁵ and some types of SWCNT networks.^{11,16-19} Burke and co-workers measured the microwave conductivity of individual SWCNTs and investigated their operation as a transistor at 2.6 GHz.^{13,14} For SWCNT networks with 30 nm thickness, our previous work finds that the ac conductivity is frequency independent up to an onset frequency $\omega_0/2\pi$ of about 10 GHz, beyond which it increases with an approximate power law behavior.¹⁷ For thicker films with thickness in the range of tens of micrometers, Petit *et al.* found that conductivities at dc and 10 GHz are almost the same.¹¹ Fu-

hrer *et al.* observed the nonlinearity of the electric-field-dependent conductivity of relatively thick nanotube networks, and they claimed that the charge carriers can be localized by disorder in the SWCNTs with an approximate length scale l_{loc} of 1.65 μm .^{18,19} Skakalova *et al.* studied the current-voltage (I - V) characteristics of individual nanotubes and nanotube networks of varying thickness, and discussed the modulation of I - V characteristics by a gate-source voltage.¹² However, there is a lack of frequency- and electric-field-dependent conductivity investigation for systematic variation of network densities, and also there is no correlation study between the onset frequency ω_0 and the length scale determined from nonlinear transport.

The frequency- and electric-field-dependent conductivity investigation of different network densities is not only helpful to build a comprehensive understanding of the electrical transport properties of SWCNT networks, but is also important for the sake of applications of these networks.^{17,20,21} For example, when using SWCNT networks to construct high speed transistors, or as transparent shielding materials, knowledge of their frequency-dependent electric transport properties are required. Also, use of SWCNT networks as interconnects in circuits requires understanding of their electric-field-dependent properties.

In this paper, we investigated the frequency- and electric-field-dependent conductivity for SWCNT networks with systematically varying densities. We find that the onset frequency ω_0 extracted from the frequency dependent measurement increases with the film thickness, while the length scale extracted from the electric-field-dependent measurement decreases at the same time. Using the measured ω_0 and the extracted length scale L_E for different films, we developed an empirical relation between the two transport measurement methods.

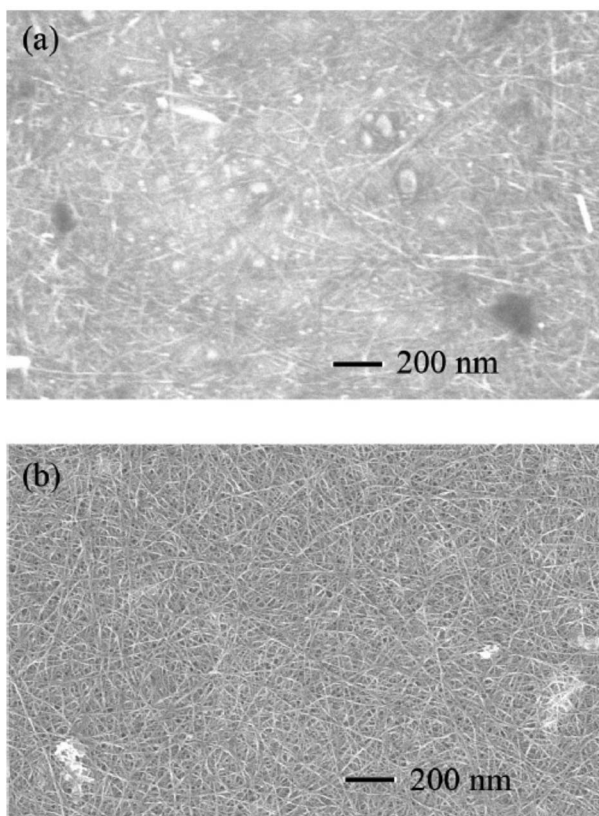


FIG. 1. SEM of two SWCNT network samples with different densities: (a) submonolayer nanotube film and (b) nanotube film with thickness of about 20 nm.

II. SAMPLES AND EXPERIMENTAL SETUP

SWCNT networks on polyethylene terephthalate substrate are prepared by the spraying method.²² Arc-discharged nanotube powder from Carbon Solution Inc. was dispersed in water with sodium dodecyl sulphate surfactants. The tubes were purified with nitric acid and left with a variety of functional groups.²² After the nanotubes were sprayed on the substrate, the samples were rinsed in water thoroughly to wash away the surfactant. The network density, defined as the number of nanotubes per unit area, was controlled by the solution concentration (0.1–1 mg/mL) and the spraying time (10–60 s). The nanotubes formed bundles with size of 4–7 nm and length of 2–4 μm .²³ The thicknesses of the films range from submonolayer to 200 nm, corresponding to room temperature sheet conductance ranging from 10^{-6} to 10^{-2} S/square. Figure 1 shows scanning electron microscopy (SEM) images of films with two different coverage densities. It is convenient to characterize the films by their sheet conductance rather than conductivity, because of the inhomogeneous nature of the conducting pathways and, thus, the difficulty in assigning a film thickness, particularly for submonolayer films.

The Corbino reflectometry setup, which is ideal for broadband conductivity measurements of resistive materials,^{24–26} was used to investigate the conductivity of the SWCNT networks. The measurement procedures are similar to our previous work.¹⁷ In order to measure the conductivity in as

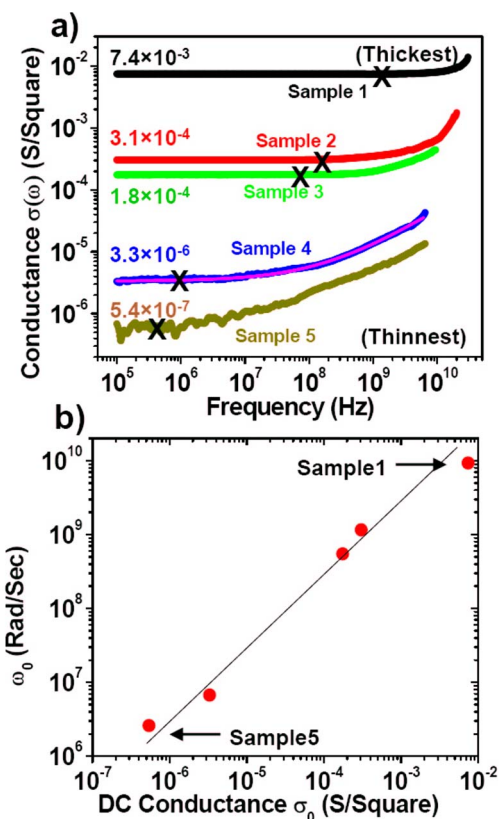


FIG. 2. (Color online) (a) Real parts of the ac conductance for samples with different densities at room temperature. The black crosses mark the fit onset frequency ω_0 for each curve. The magenta (gray) line is the typical fit result of the extended pair approximation model for sample 4 with $\sigma_0=3.3 \times 10^{-6}$ S/square, $\omega_0=1.1 \times 10^6$ rad/s, $k=0.12$, and $s=0.52$. (b) The onset frequencies vs dc conductance of SWCNT networks. The solid line has a slope of 1.

broad a frequency range as possible, two test instruments are used, the Agilent E8364B network analyzer (covering 10 MHz–50 GHz) and the Agilent 4396B network analyzer (covering 100 kHz–1.8 GHz), giving five and a half decades of frequency coverage. The electric-field-dependent conductivity was measured with a standard four-probe method in a well-shielded high precision dc transport probe.²⁷

III. FREQUENCY-DEPENDENT CONDUCTIVITY

The data of conductance vs frequency are shown in Fig. 2(a). The films decrease in thickness from sample 1 (200 nm) to sample 5 (submonolayer). For all the films, the real parts of the conductance keep their dc value up to a characteristic frequency and start to increase at higher frequency. This kind of behavior has been widely observed for disordered systems.^{28–30} Similar behavior has been found for carbon nanotube polymer composites close to the percolation threshold, in which the extended pair approximation model was applied to describe the observed phenomena.^{31,32} The carbon nanotube networks in Fig. 2(a) have densities well above the percolation threshold. However, since the junction

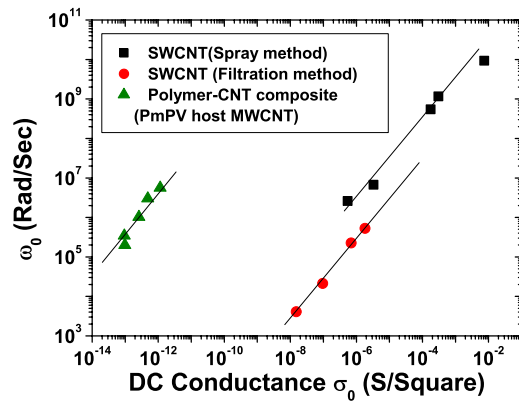


FIG. 3. (Color online) The onset frequency vs dc conductance for different SWCNT networks at room temperature. The three solid lines all have a slope of 1.

resistances between different tubes are much larger than the resistance of the tubes themselves,^{7-9,16} SWCNT networks above the percolation threshold can still be seen as systems with randomly distributed barriers for electrical transport. In this case, the extended pair approximation model can be used to describe the real part of the ac conductance:

$$\sigma = \sigma_0 [1 + k(\omega/\omega_0)^s], \quad (1)$$

where σ_0 is the dc conductance, $s \leq 1.0$, k is a constant, and ω_0 is the onset frequency.³¹

The frequency-dependent conductance in Fig. 2(a) fits well to the extended pair approximation model. Figure 2(b) shows the relation between the fit film onset frequency and the dc sheet conductance. The onset frequency changes from 2×10^6 to 1×10^{10} rad/s as the sheet conductance increases from 10^{-6} to 10^{-2} S/square. The onset frequency of the ac conductance increases as the dc conductance increases. The solid line in Fig. 2(b) has a slope of 1, implying a linear relation between the onset frequency and their dc sheet conductance, or $\omega_0 \sim \sigma_0$, over about four decades.

We also measured the frequency-dependent conductance of ultrathin submonolayer nanotube networks, which are fabricated via the filtration method.⁵ We choose chloroform as the solvent instead of water to avoid the washing steps which can easily destroy the submonolayer film structure. The network density is controlled by the concentration and volume of the solvent used.⁵ The conductance of these films are measured by a 4284A Precision LCR meter, covering the frequency range from 20 Hz to 1 MHz. For these films just above the percolation threshold, their frequency-dependent conductance also fits well to the extended pair approximation model. In Fig. 3, we plot the onset frequency versus their dc sheet conductance. For comparison, we also present results of Kilbride *et al.*³¹ for polymer-nanotube composites as well as the data from Fig. 2(b) for our films prepared by the spray method. The three solid lines in Fig. 3 all have a slope of 1 (rad/s S). Here, an interesting result is that although the intercepts are very different, the slopes of the three different samples are essentially the same. The difference in intercept is due to the different types of nanotubes. Different carbon nanotube sources have different bundle sizes and lengths,

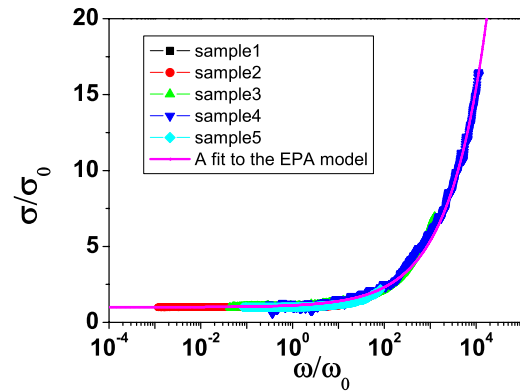


FIG. 4. (Color online) Master scaling curve showing the ac conductance for SWCNT network samples (spray method) with different densities at room temperature. The red (gray) solid line is a fit to the extended pair approximation model $k=0.12$ and $s=0.52$.

which causes the conductance difference. The polymer-carbon nanotube (CNT) composite has much smaller dc conductance than the other two, due to the separation of SWCNTs by polymer that leads to charge transfer barriers. Despite these differences in detail, there is a universal relationship between onset frequency and dc conductance.

The linear proportionality $\omega_0 \sim \sigma_0$ is one of the characteristic features of ac conductance of disordered solids.³⁰ For disordered systems, the universality of ac conductance has been studied by many researchers since its discovery in the 1950s, and is usually referred to as the Taylor-Isard scaling.²⁸⁻³⁰ This inspires us to investigate the scaling behavior of the conductance and frequency for SWCNT networks. Similar to the work of Kilbride *et al.*,³¹ taking the dc conductance σ_0 and the onset frequency ω_0 as scaling parameters, we plotted the ac conductance data for all samples in Fig. 4. The data show a scaling behavior, with all data sets falling on the same master curve described by $k=0.12$ and $s=0.52$.

In order to explain the observed onset frequency change with the SWCNT volume fraction for polymer-nanotube composites close to percolation threshold, Kilbride *et al.* defined a characteristic length scale, the ‘‘correlation length’’ ξ .³¹ For our samples, which are well above the percolation threshold, we can similarly define the correlation length ξ as the distance between connections in the sample, i.e., the distance between junctions of the multiply connected SWCNT network. When one measures the conductance at a given frequency, there is a typical probed length scale. At low frequencies (corresponding to long time periods), the carriers travel long distances in one-half ac cycle and the experiment investigates longer length scales. At high frequencies, the carriers travel short distances in one-half ac cycle and the probed length scale is shorter. In the absence of an applied dc electric field, and assuming a random walk, the probed length scale $L_\omega \propto \omega^{-1/2}$.³¹

For low frequency, $L_\omega > \xi$, the probed length scale spans multiple junctions of the SWCNT network. The junction resistances between different tubes are much larger than the resistances of the tubes themselves.^{7-9,16} Hence, the conductance is small and equal to the dc conductance. As the fre-

quency increases, L_ω becomes smaller than ξ , $L_\omega < \xi$, and the junction resistances have less contribution to the total resistance. The intrinsic properties of the SWCNT then dominate the measurement. Therefore, the observed conductance increases as the frequency increases. The transition frequency is expected to be that where carriers scan an average distance of order of the correlation length.³¹

The SWCNT film can be treated as a random walk network, in which the probed length scale at a given frequency goes as $L_\omega \sim \omega^{-1/2}$. Then with the onset frequency ω_0 of the samples, we are able to estimate their correlation length $\xi \approx L_{\omega_0} \propto \sqrt{\frac{1}{\omega_0}}$. As the density of the SWCNT networks increases there are more junctions and the average distance between connections, the correlation length ξ , becomes smaller and thus the onset frequency ω_0 increases. This is consistent with the behavior shown by the data in Fig. 2.

IV. ELECTRIC-FIELD-DEPENDENT CONDUCTIVITY

From the measured frequency-dependent conductivity, we observed that the correlation length ξ varies as the thickness of the film increases. Due to the large resistance of junctions between different tubes, the carriers in the SWCNT networks are easier to move on small length scales than on larger length scales. This phenomenon inspires us to investigate whether the transport properties are nonlinear as a result. According to the works of Fuhrer *et al.*, the localization behavior of a SWCNT network can be studied by measuring the electric-field-dependent nonlinearity of the conductivity.^{18,19} Generally, increasing both the temperature and the electric field reduces the effects of localization. Hence, a system typically displays a characteristic electric field at which nonlinear conductivity begins to appear. Through measurement of the characteristic field E_c , one can determine a length scale of the system:

$$L_E = \frac{k_B T}{e E_c}, \quad (2)$$

where L_E corresponds to the size of the regions with good conductivity, and eEL_E is the energy gained by a carrier in one conducting region on average.^{33,34} For our SWCNT films, L_E depends on the average distance between connections and, thus, should vary with sample thickness. For relatively thick films ($\sim 10 \mu\text{m}$) with low sheet resistance, Fuhrer *et al.* found a temperature-independent length scale $l_{loc} \sim 1.65 \mu\text{m}$ in a SWCNT film.^{18,19}

Here, we investigated the electric-field-dependent conductance for a different class of films. The studied samples were cut into rectangular pieces with length $\sim 8 \text{ mm}$ and width $\sim 3 \text{ mm}$. Gold contact leads, which completely cover the width of the samples, were deposited on the surfaces of the samples to form a standard four-probe pattern. The measured SWCNT networks have dimensions of $\sim 3.5 \times 3 \text{ mm}^2$ between the two voltage leads. Because SWCNT films have a large in-plane thermal conductivity,^{35,36} and the probe used to perform the measurement was specially designed to reduce heating effects,²⁷ we believe that the heating effect can be ignored in our measurement range. This was confirmed by

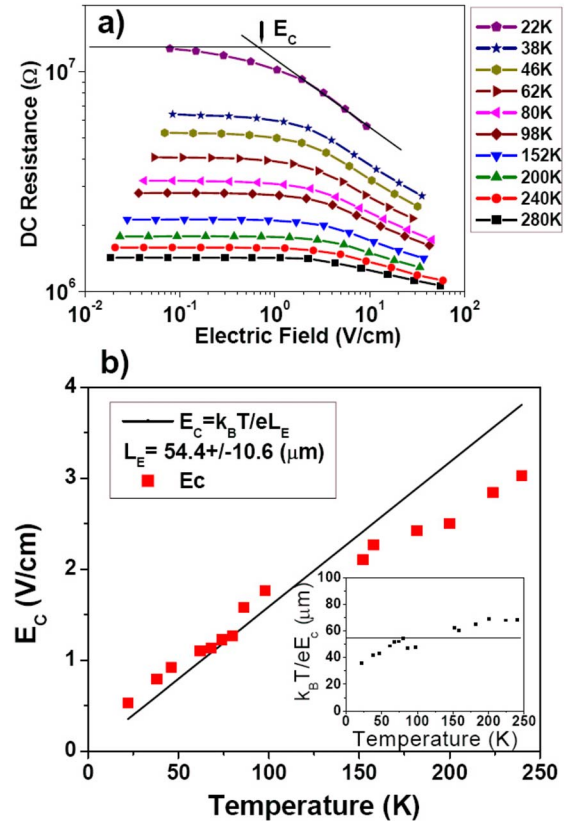


FIG. 5. (Color online) (a) dc resistance vs electric field for a submonolayer (sample 5) SWCNT network at different temperatures. (b) E_c vs temperature and extracted length scale for this sample.

observing the voltage response of pulsed current input of several samples in the time domain with an oscilloscope.

The dc resistance vs electric field of a submonolayer film (sample 5) at different temperatures is shown in Fig. 5(a). We can see clearly that there is nonlinear behavior even at room temperature. As sketched in Fig. 5(a), we extracted E_c for each temperature, which is the characteristic electric field at which nonlinear conductance begins to appear.¹⁸ Figure 5(b) shows the extracted E_c vs temperature for this sample. As temperature increases, E_c also increases. Roughly, E_c and temperature have a linear relationship and satisfy the equation $E_c = k_B T / e L_E$, with $L_E \approx 54 \mu\text{m}$. Note that this is much larger than the l_{loc} obtained in Refs. 18 and 19. This suggests that a different mechanism for hindering transport is active here, namely, poor contacts between bundles of SWCNTs.

To investigate the dependence of L_E on the film thickness, we measured the electric-field-dependent conductance for samples with various thicknesses. We found that the nonlinear behavior strongly depends on the thickness of the film. At low temperature, all the samples show nonlinear behavior of resistance on electric field, and the critical field E_c is larger for thicker samples and smaller for thin samples. At room temperature, all the other samples are purely Ohmic (linear) in electric fields up to 100 V/cm, except for the thinnest sample (sample 5), which showed electric-field-dependent conductance at all temperatures. Through the critical field E_c , we extracted the L_E for different density films, shown in Fig.

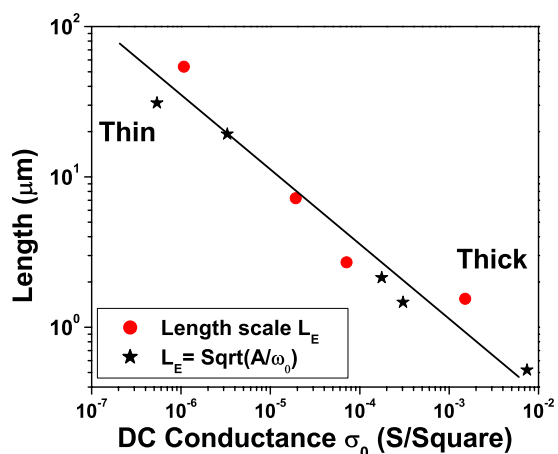


FIG. 6. (Color online) Comparison of the length scale L_E obtained from electric-field-dependent dc conductance data (red dot) and the estimated length scale from frequency-dependent conductance measurement $\sqrt{A/\omega_0}$ (black star) of SWCNT networks of various densities. The line has slope $-1/2$ in the log-log plot.

6 as red dots. Clearly, L_E depends on the density of the SWCNT networks. For the thicker film with larger SWCNT density, which has larger sheet conductance, the L_E is smaller. The lower density films with larger average distance between the junctions has larger L_E .

Although the localization behavior may be affected by the properties of individual SWCNTs,^{18,19} the above result shows that the observed behavior is more likely a consequence of poor electric conduction through interbundle junctions. As the thickness and density increase, there are more and more connections, which decreases the length scale L_E , as shown in Fig. 6.

When the film thickness increases to a large value, the density of the SWCNTs and connections of the film will finally saturate and stop increasing. For those very thick SWCNT films (also called mats), their correlation length ξ and also the length scale L_E , as well as the onset frequency, will be independent of the thickness, but depend on the properties of individual bundles, which include both the disorder of the individual nanotube and also the geometry of the bundles. Hence, the difference of SWCNT sources and purities can change the onset frequency. We believe this is the reason that our previous work found that the ac conductivity follows the extended pair approximation model with an onset frequency ω_0 of about 10 GHz, while Petit *et al.* found that SWCNT networks have the same conductivities at dc and 10 GHz for SWCNT networks with thickness in the range of tens of micrometers.^{11,17}

V. DISCUSSION

The frequency-dependent conductivity shows that the onset frequency ω_0 increases with the sample thickness and gives an estimation of the correlation length ξ of the sample, $\xi \sim L_{\omega_0} \propto \sqrt{\frac{1}{\omega_0}}$. ξ and L_{ω_0} decrease as the sample thickness increases. The dc nonlinear conductivity measurement shows that the length scale L_E of the samples also decreases with

increasing sample thickness. Qualitatively, L_{ω_0} and L_E have the same dependence on the sample thickness. Based on the above consideration, it is reasonable to expect some correlation between the onset frequency ω_0 and the length scale L_E , and we proposed the following relation:

$$L_E = \sqrt{\frac{A}{\omega_0}}, \quad (3)$$

where A is a fitting parameter, which can be obtained from our experiment data, $A \sim 2.5 \pm 0.5 \times 10^{-3} \text{ m}^2/\text{s}$. Figure 6 shows the comparison of the nonlinear transport length scale L_E measured directly through electric-field-dependent dc conductance measurements (red dot) and the right-hand side of Eq. (3) from the frequency-dependent measurement (black star). They are consistent with each other. In this way, we obtain an empirical relation between the frequency-dependent and electric field-dependent conductivity. The parameter A should depend on the diffusion properties of carriers in the SWCNT films.³⁷ Writing $L_E = \sqrt{4Dt^*}$, where D is a diffusion constant and t^* is the corresponding time scale, we take $D = A/8\pi$. Assuming the Einstein relation $\mu = \frac{De}{k_B T}$, we can estimate the mobility of carriers on the SWCNT network, which is on the order of $10^{-2} \text{ m}^2/\text{V s}$. This is much smaller than that of the individual single-walled carbon nanotube, which can be on the order of $10^0 - 10^1 \text{ m}^2/\text{V s}$ at room temperature.^{38,39} In the SWCNT networks, due to the randomly distributed barriers for electrical transport, the mobility is expected to be much smaller than the SWCNT itself. The carbon nanotube film-based transistors have reported mobilities on the order of $10^{-4} - 10^{-1} \text{ m}^2/\text{V s}$,^{20,40,41} which is consistent with our estimation. To get a deeper physical understanding of these networks, more investigation and theoretical work are needed. For example, measuring the temperature dependence of the frequency-dependent conductivity for SWCNT networks with various densities would be one approach.^{11,17}

VI. CONCLUSION

To conclude, we systematically studied the frequency- and electric-field-dependent conductivity of SWCNT films of various thicknesses. We found that the poor interbundle junctions affect the transport behavior of the carriers in the SWCNT films, which causes strong thickness dependence of characteristic length scales. A thinner film has larger correlation length ξ and length scale L_E , so it has a smaller onset frequency ω_0 , whereas a thicker film with smaller correlation length ξ and length scale L_E has a larger onset frequency ω_0 . An approximate empirical formula relating the onset frequency ω_0 and nonlinear transport length scale establishes contact between the frequency- and electric-field-dependent conductivity, which helps us to understand the electric transport properties of the SWCNT films.

ACKNOWLEDGMENTS

The authors would like to thank M. S. Fuhrer, C. J. Lobb, Weiqiang Yu, and Bing Liang for their help and discussions

on this work. This work has been supported by Center for Nanophysics and Advanced Materials of the University of Maryland and the National Science Foundation Grants Nos. DMR-0404029, DMR-0322844, and DMR-0302596.

*umdxuhua@gmail.com

- ¹G. Grüner, *J. Mater. Chem.* **16**, 3533 (2006).
- ²P. M. Ajayan and O. Z. Zhou, *Carbon Nanotubes: Synthesis, Structure, Properties and Application* (Springer, Berlin, 2001).
- ³R. H. Baughman, A. A. Zakhidov, and W. A. de Heer, *Science* **297**, 787 (2002).
- ⁴D. Zhang, K. Ryu, X. Liu, E. Polikarpov, J. Ly, M. E. Tompson, and C. Zhou, *Nano Lett.* **6**, 1880 (2006).
- ⁵L. Hu, D. S. Hecht, and G. Grüner, *Nano Lett.* **4**, 2513 (2004).
- ⁶M. S. Dresselhaus, G. Dresselhaus, and P. C. Eklund, *Science of Fullerenes and Carbon Nanotubes* (Academic, San Diego, CA, 1996).
- ⁷M. S. Fuhrer, J. Nygard, L. Shih, M. Forero, T. Yoon, M. S. C. Mazzoni, H. J. Choi, J. Ihm, S. G. Louie, A. Zettl, and P. L. Mcueen, *Science* **288**, 494 (2000).
- ⁸A. B. Kaiser, G. Dusberg, and S. Roth, *Phys. Rev. B* **57**, 1418 (1998).
- ⁹M. Stadermann, S. J. Papadakis, M. R. Falvo, J. Novak, E. Snow, Q. Fu, J. Liu, Y. Fridman, J. J. Boland, R. Superfine, and S. Washburn, *Phys. Rev. B* **69**, 201402(R) (2004).
- ¹⁰J. E. Fischer, H. Dai, A. Thess, R. Lee, N. M. Hanjani, D. L. Dehaas, and R. E. Smalley, *Phys. Rev. B* **55**, R4921 (1997).
- ¹¹P. Petit, E. Jouguelet, J. E. Fischer, A. G. Rinzler, and R. E. Smalley, *Phys. Rev. B* **56**, 9275 (1997).
- ¹²V. Skakalova, A. B. Kaiser, Y. S. Woo, and S. Roth, *Phys. Rev. B* **74**, 085403 (2006).
- ¹³Z. Yu and P. J. Burke, *Nano Lett.* **5**, 1403 (2005); S. Li, Z. Yu, S. Yen, W. C. Tang, and P. J. Burke, *ibid.* **4**, 753 (2004).
- ¹⁴P. J. Burke, *IEEE Trans. Nanotechnol.* **2**, 55 (2003).
- ¹⁵M. Zhang, X. Huo, P. Chan, Q. Liang, and Z. K. Zhang, *Appl. Phys. Lett.* **88**, 163109 (2006).
- ¹⁶A. B. Kaiser, K. J. Challis, G. C. McIntosh, G. T. Kim, H. Y. Yu, J. G. Park, S. H. Jhang, and Y. W. Park, *Curr. Appl. Phys.* **2**, 163 (2002).
- ¹⁷Hua Xu, L. Hu, S. M. Anlage, and G. Grüner, *Appl. Phys. Lett.* **90**, 183119 (2007).
- ¹⁸M. S. Fuhrer, M. L. Cohen, A. Zettl, and V. Crespi, *Solid State Commun.* **109**, 105 (1999).
- ¹⁹M. S. Fuhrer, W. Holmes, P. L. Richards, P. Delaney, S. G. Louie, and A. Zettl, *Synth. Met.* **103**, 2529 (1999).
- ²⁰S. J. Kang, C. Kocabas, T. Ozel, M. Shim, N. Pimparkar, M. A. Alam, S. V. Rotkin, and J. A. Rogers, *Nat. Nanotechnol.* **2**, 230 (2007).
- ²¹Z. Wu, Z. Chen, X. Du, J. M. Logan, J. Sippel, M. Nikolou, K. Kamaras, J. R. Reynolds, D. B. Tanner, A. F. Hebard, and A. G. Rinzler, *Science* **305**, 1273 (2004).
- ²²E. Bekyarova, M. E. Itkis, N. Cabrera, B. Zhao, A. Yu, J. Gao, and R. C. Haddon, *J. Am. Chem. Soc.* **127**, 5990 (2005).
- ²³L. Hu, G. Grüner, J. Gong, C.-J. Kim, and B. Hornbostel, *Appl. Phys. Lett.* **90**, 093124 (2007).
- ²⁴J. C. Booth, Dong Ho Wu, and Steven M. Anlage, *Rev. Sci. Instrum.* **65**, 2082 (1994).
- ²⁵J. C. Booth, D. H. Wu, S. B. Qadri, E. F. Skelton, M. S. Osofsky, A. Pique, and S. M. Anlage, *Phys. Rev. Lett.* **77**, 4438 (1996).
- ²⁶A. Schwartz, M. Scheffler, and S. M. Anlage, *Phys. Rev. B* **61**, R870 (2000).
- ²⁷Su Li, Ph.D. thesis, University of Maryland, 2007.
- ²⁸J. C. Dyre, *J. Appl. Phys.* **64**, 2456 (1988).
- ²⁹P. Dutta, S. Biswas, M. Ghosh, S. K. De, and S. Chatterjee, *Synth. Met.* **122**, 455 (2001).
- ³⁰J. C. Dyre and T. B. Schroder, *Rev. Mod. Phys.* **72**, 873 (2000).
- ³¹B. E. Kilbride, J. N. Coleman, J. Fraysse, P. Fournet, M. Cadek, A. Drury, S. Hutzler, S. Roth, and W. J. Blau, *J. Appl. Phys.* **92**, 4024 (2002).
- ³²D. S. Mclachlan, C. Chiteme, C. Park, K. E. Wise, S. E. Lowther, P. T. Lillehei, E. J. Siochi, and J. S. Harrison, *J. Polym. Sci., Part B: Polym. Phys.* **43**, 3273 (2005).
- ³³K. Mortensen, M. L. W. Thewalt, Y. Tomkiewicz, T. C. Clarke, and G. B. Street, *Phys. Rev. Lett.* **45**, 490 (1980).
- ³⁴N. Apsley and H. P. Hughes, *Philos. Mag.* **31**, 1327 (1975).
- ³⁵J. Hone, M. Whitney, C. Piskoti, and A. Zettl, *Phys. Rev. B* **59**, R2514 (1999).
- ³⁶Y. Ouyang and J. Guo, *Appl. Phys. Lett.* **89**, 183122 (2006).
- ³⁷P. Minnhagen, *Rev. Mod. Phys.* **59**, 1001 (1987).
- ³⁸M. S. Fuhrer, B. M. Kim, T. Dürkop, and T. Brintlinger, *Nano Lett.* **2**, 755 (2002).
- ³⁹T. Dürkop, B. M. Kim, and M. S. Fuhrer, *J. Phys.: Condens. Matter* **16**, R553 (2004).
- ⁴⁰E. Artukovic, M. Kaempgen, D. S. Hecht, S. Roth, and G. Grüner, *Nano Lett.* **5**, 757 (2005).
- ⁴¹W. Xue and T. Cui, *Appl. Phys. Lett.* **89**, 163512 (2006).